# Continuous radio-frequency heating of a model viscous solution: Influence of active current, flow rate, and salt content on temperature rise

P. Piyasena and C. Dussault

*Food Research Program, Agriculture and Agri-Food Canada, 93 Stone Road West, Guelph, Ontario, Canada N1G 5C9. Contribution No. S116 from the Food Research Program.*

Piyasena, P. and Dussault, C. 2003. **Continuous radio-frequency heating of a model viscous solution: Influence of active current, flow rate, and salt content on temperature rise.** Canadian Biosystems Engineering/Le génie des biosystèmes au Canada **45**: 3.27-3.34. Radio frequency can induce molecular friction in food products resulting in an internal heating effect; therefore, better heating of sensitive liquid food products can be obtained. A study was conducted to investigate the influence of active current (275-490 mA), flow rate (12-48 L/h) and salt content (0-0.7%) on the heating of a model viscous 0.27% guar solution in a 1.5 kW radio frequency heater on the temperature rise during continuous heating. The temperature increase ($\Delta T$) was inversely proportional to the flow rate. A linear relationship was found between the active current and $\Delta T$. The effect of salt content was not significant within the range tested. Based on the data obtained, an empirical model was developed to predict $\Delta T$. The radio-frequency heater can provide enough energy to heat the viscous products up to 86°C under tested conditions. The flow in the holding tube was laminar under the tested conditions for 0.27% guar solution. The maximum power efficiency that could be achieved was 39%. **Keywords:** radio frequency, heating, flow rate, active current, salt, guar.

Les produits alimentaires exposés aux radiofréquences subissent un réchauffement interne causé par le frottement entre leurs molécules constituantes. En conséquence, un meilleur réchauffement de produits alimentaires liquides et délicats peut être obtenu. Une étude a été réalisée pour déterminer l'influence d'un courant actif (275-490 mA), du débit (12-48 L/h) et de la teneur en sel (0-0,7%) sur le chauffage d'une solution visqueuse de guar à 0,27% par un réchaud à radiofréquence d'une puissance de 1,5 kW et l'effet sur l'augmentation de la température durant un chauffage continu. L'augmentation de la température ($\Delta T$) était inversement proportionnelle au débit. Une relation linéaire a été établie entre le courant actif et $\Delta T$. L'effet de la teneur en sel n'était pas significatif dans la plage de concentrations testées. Un modèle empirique a été développé pour prédire $\Delta T$ à l'aide des données recueillies. Sous les conditions de l'étude, le réchaud à radiofréquence peut fournir assez d'énergie pour chauffer les produits visqueux jusqu'à 86°C. Le débit dans les tubes de rétention était laminaire pour la solution de guar à 0,27% et pour les conditions des essais. Une efficacité énergétique maximale de 39% a pu être atteinte. **Mots clés**: radiofréquence, chauffage, débit, courant actif, sel, guar.

## INTRODUCTION

Pumpable food products are most commonly pasteurized by means of heat exchangers in which heat is transferred across a metal surface and into the product. Radio-frequency (RF, 3 kHz-300 MHz, Ryynänen 1995) induces molecular friction in the product which causes internal heating. In RF heating, the product to be heated forms a dielectric between two metal capacitor plates that are charged alternatively positive and negative by a high frequency electric field. Polar molecules such as water try to align themselves with the polarity of the plates. Since the polarity of the plates is changed rapidly (for the RF frequency of 27 MHz, $27 \times 10^6$ times/s), the molecules try to realign themselves continuously thereby generating heat due to friction.

RF has been successfully used for moisture removal, tempering after baking, and thawing of meat (Anonymous 1993; McCormick 1988). However, until recently application of RF technology for liquid foods has not been adequately investigated. Demeczky (1974) successfully showed that juices (peach, quince, and orange) in bottles moving on a belt through an RF applicator had better bacteriological and organoleptic quality than juices treated by conventional thermal methods. However, as most liquid foods are now aseptically processed and packaged, development of continuous RF processing would be attractive to the industries. Houben et al. (1991) used RF to pasteurize sausage emulsion continuously in a bench-top RF heater. It was demonstrated by Geveke et al. (2002) that there were no non-thermal microbial effects of RF energy nor were there any synergistic effects of RF energy with heat. Thus, thermal effect is the main reason for inactivation of microorganisms during RF heating.

One of the advantages of RF heating is that the product is not penetrated by the heating device, and the electrode applicator system is completely external to the product zone. Therefore, contamination is minimized and cleaning of the system is not required except for the applicator tube (Koral 1996). Other advantages of RF heating include: rapid and uniform heating; high penetration depth; short residence time; no heat transfer surfaces; saving of process time, space, and labor; reduced noise level; application to different product geometry and sizes; clean-in-place is possible; improved product quality; and no need to use molds in which the meat products are placed when heating in hot water. In comparison to microwave (MW, 300MHz - 300GHz, Ryynänen 1995), RF does not suffer from the uneven heating and lack of penetration

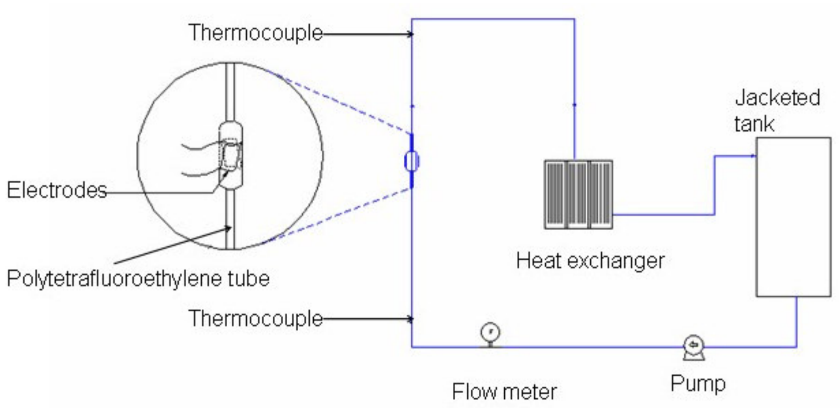


**Fig. 1. Schematic presentation of radio frequency heating experimental set-up.**

depth characteristic of most MW heating systems. Therefore, RF heating can be a potential alternative method for heating viscous and/or heat sensitive liquid food, and pharmaceutical and specialized products such as nutraceuticals and functional food ingredients.

Work in our laboratory has focused on the development of RF based heating methods for liquid and solid foods (Awuah et al. 2002; Laycock et al. 2003). The present study will extend the previous work to the continuous RF heating for heat sensitive products such as liquid egg products that are viscous and non-Newtonian. Guar solution was selected as a model liquid for this study. Thus, the objectives of this study were (1) to determine the influence of various operational parameters such as flow rate, active current, and salt content on the temperature increase of a model solution; and (2) to analyse the power absorption and efficiency during continuous radio-frequency heating.

## MATERIALS and METHODS

### RF heating system

The RF heating system that was used in this study is illustrated in Fig. 1. The 1.5 kW RF heater (Strayfield Ltd., Reading, UK) has two components; the RF generator and the applicator circuit (Strayfield 1993). The RF energy is produced by the generator which is comprised of an oscillator, transformer, rectifier, and a 'tank circuit' having inductive and capacitive components. The tank circuit was designed to have a frequency of 27.12 MHz. The applicator circuit has an applicator tube, two electrodes, tuning capacitor plates, and an inductance coil. The applicator tube, or process tube, through which the product flows is made of polytetrafluoroethylene (PTFE). The original tube (97 mm ID), which was made for particulate foods, was modified to be used for liquid foods. The original diameter of the heating section was kept in order to supply the maximum possible power from the electrodes, and the other section was reduced to 25.4 mm (ID) to increase the flow rate. The smaller diameter permitted better control of the holding time for a HTST process, especially during experimental runs. Two helical electrodes were placed outside the larger section of the applicator tube (Figs. 1 and 2). These electrodes form, in effect, two capacitor plates. The product flowing in the tube becomes the dielectric.

The RF power applied to any product during processing can be decreased or increased by reducing or increasing the gap between the plates of the tuning capacitor. This is done manually or automatically from outside using a gear mechanism. Alternatively, the power level could be raised by increasing the inductance in the applicator. This is achieved by increasing the length of the tuning inductance coil. The current passing through the product (active current) ranges from 0 - 500 mA, above which the arc trip unit will be activated to temporarily disable the heater. The standing current, the current needed to maintain the oscillations of the RF field when the applicator tube is empty, is 175 mA. The actual current which is used to produce heat in the product is the difference between the ammeter reading (active current) and 175 mA. To obtain the power input of the RF heater, the actual current has to be multiplied by the high voltage, which is approximately 4.6 kV for this unit.

### Experimental set-up

A positive displacement pump (Pureflo 24 series lobe gear pump, Type: S2, Model: 24950-1370, ITT Jabsco, Hoddesdon, Herfordshire, England) controlled by a digital display variable drive (Model: SP500, Reliance Electric, Athens, GA) was used to pump the solution from the jacketed tank to the applicator tube (Fig. 1). The product was heated in the heating section of the applicator tube then cooled in the cooling section of a plate

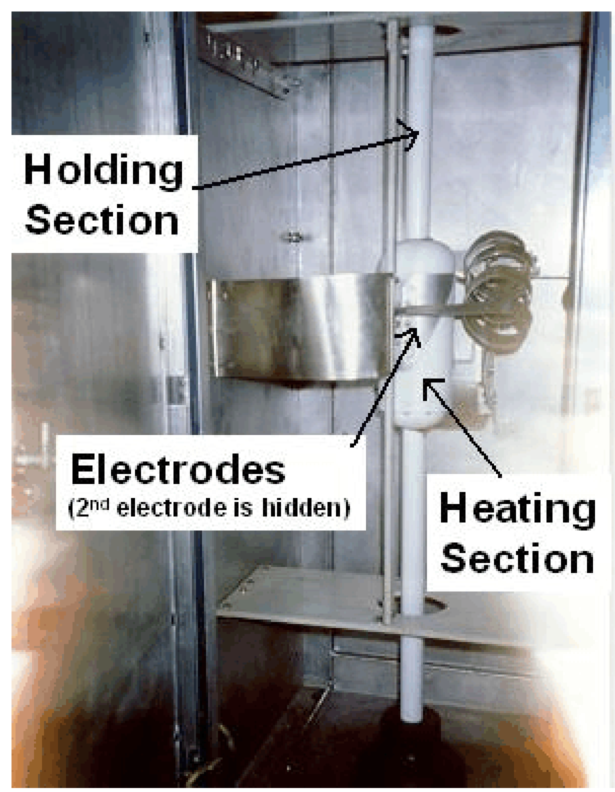


**Fig. 2. Illustration of electrodes, applicator tubes, and holding section of an RF heater.**

heat exchanger (Junior Paraflow, APV, Woodbridge , ON). The plate heat exchanger was only used for cooling the product. A magnetic flow meter (Model: M900, Krone, Sliedrecht, The Netherlands) and a pressure gauge were placed between the pump and the applicator tube to measure the flow rate and to monitor the pressure, respectively.

**Instrumentation and data acquisition**

Two thermocouples (Type T, SKYL-Tech. Inc., North Plainfield, NJ) were used to measure the inlet and outlet temperatures (Fig. 1). The current passing through the product (active current) was measured using a digital ammeter and the flow using a magnetic flow meter. All four sensors were connected to a data logger (DR 230, Yokogawa, Tokyo, Japan). The cables were shielded (CM1PR24, Belden, Richmond, IN) to prevent noise and disturbance. The data acquisition was done using Darwin Basic software (DP200-13, Yokogawa, Tokyo, Japan) and imported into a spread sheet software program (Lotus 1-2-3, Rel.5, Lotus Develop. Corp., Cambridge, MA) for further analysis.

**Solution preparation**

Each 200 kg guar solution contained 540 g (0.27% w/w) of guar (Dycol 4500F, Rhodia, Cranbury, NJ) and its respective amount of salt (0.20, 0.45, 0.70%). The density and specific heat of 0.27% guar solution at 20°C were 1003.54 kg/m$^3$ and 4450 J kg$^{-1}$ °C$^{-1}$, respectively. The guar powder was divided into five parts and was thoroughly mixed with the 1.6 kW mixer (IKA Ultra-Turrax T65DPX, Janke & Kunkel GmbH, Staufen, Germany) into five containers, each filled with 20 L of water. The containers were emptied into the jacketed tank and additional water was added to obtain 200 kg of solution. The solution was stirred and the salt was slowly added. To ensure the complete hydration of the guar powder, the solution was stirred for at least 15 h at 4°C before testing.

**Rheological properties of guar solution**

The maximum shear rate at the wall in the heating and holding section was 8.3 s$^{-1}$ at the tested maximum flow rate of 48 L/h. Guar solution (0.27%) is a non-Newtonian fluid (Piyasena and McKellar 1999a) and the power-law model (Eq. 1) was fitted for the shear rate and shear stress data obtained from the shear rate sweeps from 0 - 25 s$^{-1}$ using a Bohlin CVO-50 viscometer (Bohlin, Cranbury, NJ) equipped with a 40-mm cone and plate (cone angle = 4°C). Experimental procedure and the calculation steps are described by Piyasena and McKellar (1999b). Shear rate sweeps were made at 5, 20, 35, 50, and 65°C in triplicates.

$$\sigma = m\gamma^n \tag{1}$$

where:

σ = shear stress (Pa),
γ = shear rate (s$^{-1}$),
m = consistency coefficient (Pa.s$^n$), and
n = power law index.

The "Table Curve," curve fitting software (Version: 3.12, Jandel Scientific, San Rafael, CA) was used to analyze the data.

To characterize the type of flow in the holding tube, the Generalized Reynolds number ($N_{GRe}$) was calculated using Eq. 2 (Sakiadis 1984; Rao and Anantheswaran 1982).

$$N_{G\mathrm{Re}} = \frac{\rho D^n v_{av}^{2-n}}{m 8^{n-1}\left(\frac{3n+1}{4n}\right)^n} \tag{2}$$

where:

ρ = density (kg/m$^3$),
D = diameter of holding tube (m), and
$v_{av}$ = average velocity (m/s).

The maximum velocity ($v_{max}$) was used to calculate the minimum residence time ($RT_{min}$) in the holding tube. The relationship between average velocity, $v_{av}$, and $v_{max}$ that is found in the center of the tube was calculated using Eq. 3 for laminar non-Newtonian flow (Palmer and Jones 1976).

$$\frac{v_{av}}{v_{\max}} = \frac{1+n}{1+3n} \tag{3}$$

where:

$$v_{av} = Q / A \tag{4}$$

Q = volumetric flow rate (m$^3$/s), and
A = cross sectional area of holding tube (m$^2$).

By calculating the $v_{max}$, minimum residence time, $RT_{min}$ can be calculated using Eq. 5.

$$RT_{\min} = L / v_{\max} \tag{5}$$

where: L = length of holding tube (m).

**Power generation and absorption during RF heating**

A simplified model to calculate the power generated during RF heating was proposed by Koral (1996) and is given in Eq. 6.

$$P_w = (AcC - 0.175)V \tag{6}$$

where:

$P_w$ = power generated (W),
AcC = active current (A), and
V = high voltage across the electrodes.

The input power was calculated from the actual current and the high voltage of the RF unit. The actual current is the difference between the active current and the standing current of 175 mA (Strayfield 1993). The high voltage across the electrodes for this RF unit has been estimated to be 4600 V (Strayfield 1993).

Power absorbed by the product during continuous steady flow could also be calculated using Eq. 7 (Strayfield 1993).

$$P_w = Q\rho C_p \Delta T \tag{7}$$

where:

$C_p$ = specific heat (J kg$^{-1}$ °C$^{-1}$), and
ΔT = temperature rise (°C).

By rearranging the variables and substituting Eq. 6 for $P_w$, Eq. 7 becomes:

$$\Delta T = \frac{(AcC - 0.175)V}{C_p Q \rho} \tag{8}$$

Power efficiency ($P_{efficiency}$, %) of the RF heater could be calculated as described by Houben et al. (1991) as:

$$P_{efficiency} = 100\frac{P_w}{P_s} \quad (9)$$

where: $P_s$ = power supplied to generator from main (W).

The maximum $P_s$ for this RF heater is 3.2 kW (Strayfield 1993). The correction factor and percentage error for ΔT were calculated using Eqs. 10 and 11, respectively.

$$Correction\ factor\ for\ \Delta T = \frac{Measured\ \Delta T}{Calculated\ \Delta T\ (Eq.8)} \quad (10)$$

$$Percent\ Error\ for\ \Delta T = \frac{Calculated\ \Delta T\ (Eq.8) - Measured\ \Delta T}{Measured\ \Delta T} \times 100 \quad (11)$$

**Experimental procedure**

The solution was pumped through the system at selected flow rates (12, 24, 30, and 48 L/h). The heater was activated and set at a selected active current (275, 325, 375, 425, and 490 mA). The solution travelling through the system was heated in the vertical applicator tube, then passed through the holding tube, and cooled in the heat exchanger. When the outlet temperature at the top of the applicator tube had reached equilibrium and remained constant ± 0.1°C for 3 minutes, data were collected, then the active current was increased to the next level, 325 mA. The outlet temperature was allowed to rise until it reached a constant temperature for the selected operational parameters. Three data points were obtained for each set of operational conditions. The experiments were carried out for three salt concentrations (0.2, 0.45, and 0.70%).

**Data analyses and mathematical modelling**

Mathematical models have already been developed to estimate the temperature rise during RF heating (Orfeuil 1987). However, these models require that the dielectric properties of the materials and the electric field between the electrodes at each active current be known. Those values were not measured in this experiment. However, Eq. 8 derived from Eqs. 6 and 7 was analysed using the available data. Further, the collected data were used to develop an empirical model, specific to the studied materials, to investigate the relationship between temperature increase (ΔT) and independent variables such as flow rate, active current, and properties of foods. The maximum difference between the final and initial temperatures at equilibrium was taken as the maximum temperature increase (ΔT) generated by the RF heating at given operational conditions. The ΔTs were plotted against the flow rate, the active current, and the salt content to determine their effect. An empirical model to predict the ΔT was developed by using a multiple regression method (PROC NLIN, SAS/STAT, SAS Institute Inc., Cary, NC).

## RESULTS and DISCUSSION

**Rheological properties of guar solution**

The n and m values (Eq. 1) at different temperatures were obtained from shear stress vs shear rate plots. The regression coefficients for the power law fit were more than 0.99. Empirical equations were developed by using the least-squares method for power law index (Eq. 12, $r^2$=0.999), and consistency coefficient (Eq.13, $r^2$=0.999) as a function of temperature (T).

$$n = -0.369 - 0.0213T^{0.5} \ln T + 0.1307T^{0.5} \quad (12)$$

$$m = 0.0243 + 0.1076 \exp(-0.0577T) \quad (13)$$

The maximum $N_{GRe}$ (Eq. 2) in the holding tube at 72°C was 33.5 (D = 25.4 mm, n = 0.98, m=0.02 Pa.s$^n$, ρ = 976 kg/m$^3$, Q = 48 L/h), which is below 2100. Therefore, the flow is laminar under the tested conditions. This should be taken into consideration when the minimum residence time ($RT_{min}$) is calculated to design microbial inactivation processes using this RF heater. The $v_{max}$ (Eq. 3) at this flow rate (48L/h, $v_{av}$ = 0.026 m/s) and temperature (72°C) was 0.052 m/s. It is interesting to note that the $v_{max}$ = $2v_{av}$, which is equivalent to that of Newtonian fluid under laminar flow. It was due to the high n value (0.98) of the solution at high temperature (72°C). The $RT_{min}$ (Eq. 5) at this flow rate was L/0.052 s, where L is the length of the holding tube which can be selected for required minimum holding time.

**Influence of operational parameters on heating**

The effects of flow rate, active current, and salt concentration on the radio-frequency heating of guar solutions are given in Table 1 and plotted in Figs. 3a to 3d and 4.

**The effects of flow rate**

As expected, the ΔT decreases as the flow rate increases (Fig. 3a) for all the active currents and salt concentrations tested. This is due to the residence time of the solution which decreased by increasing the flow rate. This is consistent with the theory proposed by Orfeuil (1987) which indicated that at the slower flow rates molecules can dissipate and absorb energy in the alternating electric field for a longer period of time resulting in a greater increase in product temperature.

ΔT decreased rapidly with flow rate at the lower flow rates as shown in Fig. 3a and all the plots converged as the flow rate increased. The temperature reached at the lower flow rate may be above a certain mobility threshold after which the solution heats more rapidly. Li and Barringer (1997) reported similar observations in ham samples above 70°C. It was suggested that the increase was related to a sharp increase in the dielectric loss factor which was probably due to the protein denaturation. Likewise, the guar might have undergone changes at high temperatures which would have modified the dielectric and other thermo-physico-chemical properties. Bircan and Barringner (1997) observed that in the presence of salt the dielectric loss factor decreases dramatically with increasing viscosity.

**The effects of active current**

The ΔT increases as the active current increases at a given flow rate and salt content (Fig. 3b). When the salt content was kept constant and active current was increased, the ΔT increased linearly ($r^2$ >0.996). Generally, the ΔT increased linearly as the active current was increased for all flow rates. A similar relationship was observed by Houben et al. (1991) who found an approximately linear relationship between the ΔT and the current applied. This corresponds to the theory which states that the polarization is proportional to the field strength (Brown et al. 1947). Greater polarization leads to a greater displacement for each molecular rotation, and therefore to a greater amount of internal friction which results in a temperature increase.

**Table 1. Comparison between the experimental and the estimated temperature rise and power generation. Specific heat of each solution assumed to be constant at 4.45 kJ kg$^{-1}$ °C$^{-1}$.**

| Test | Current (A) | Salt content (%) | Flow rate (L/h) | Experimental value, ΔT (°C) | Estimated value (Eq. 8) | | | Power (W) | |
|---|---|---|---|---|---|---|---|---|---|
| | | | | | ΔT (°C) | Correction factor (Eq. 10) | Percent error (Eq. 11) | Experiment (Eq. 7) | Estimated (Eq. 6) |
| 1 | 0.490 | 0.2 | 36.6 | 28.23 | 32.03 | 0.882 | 13.44 | 1252 | 1449 |
| | | | 30 | 38.00 | 39.07 | 0.973 | 2.83 | 1381 | 1449 |
| | | | 24 | 46.87 | 48.84 | 0.960 | 4.22 | 1363 | 1449 |
| | | | 18 | 56.50 | 65.12 | 0.868 | 15.26 | 1232 | 1449 |
| | | | 12 | 86.57 | 97.69 | 0.886 | 12.84 | 1258 | 1449 |
| 2 | 0.275 | 0.2 | 27 | 12.90 | 13.78 | 0.936 | 6.84 | 422 | 460 |
| | 0.325 | | | 19.40 | 20.67 | 0.938 | 6.57 | 635 | 690 |
| | 0.375 | | | 24.60 | 27.57 | 0.892 | 12.06 | 805 | 920 |
| | 0.425 | | | 33.50 | 34.46 | 0.972 | 2.86 | 1096 | 1150 |
| | 0.490 | | | 41.17 | 43.42 | 0.948 | 5.46 | 1346 | 1449 |
| 3 | 0.275 | 0.2 | 37.2 | 8.56 | 10.00 | 0.856 | 16.86 | 386 | 460 |
| | 0.325 | | | 12.73 | 15.01 | 0.848 | 17.87 | 574 | 690 |
| | 0.375 | | | 17.57 | 20.01 | 0.878 | 13.87 | 792 | 920 |
| | 0.425 | | | 21.33 | 25.01 | 0.853 | 17.25 | 961 | 1150 |
| | 0.490 | | | 26.31 | 31.51 | 0.835 | 19.77 | 1186 | 1449 |
| 4 | 0.375 | 0.2 | 42 | 17.20 | 17.72 | 0.971 | 3.03 | 875 | 920 |
| | | | 36 | 19.78 | 20.67 | 0.957 | 4.52 | 863 | 920 |
| | | | 30 | 25.15 | 24.81 | 1.014 | 1.36 | 914 | 920 |
| | | | 22.8 | 33.89 | 32.64 | 1.038 | 3.68 | 936 | 920 |
| | | | 21 | 36.40 | 35.44 | 1.027 | 2.63 | 926 | 920 |
| 5 | 0.275 | 0.3 | 36 | 9.10 | 10.34 | 0.880 | 13.59 | 397 | 460 |
| | 0.325 | | | 13.37 | 15.51 | 0.862 | 16.00 | 583 | 690 |
| | 0.375 | | | 17.89 | 20.67 | 0.865 | 15.59 | 780 | 920 |
| | 0.425 | | | 22.39 | 25.84 | 0.866 | 15.44 | 976 | 1150 |
| | 0.490 | | | 28.26 | 32.56 | 0.868 | 15.24 | 1232 | 1449 |
| 6 | 0.275 | 0.3 | 27 | 13.76 | 13.78 | 0.999 | 0.14 | 450 | 460 |
| | 0.325 | | | 20.94 | 20.67 | 1.013 | 1.29 | 685 | 690 |
| | 0.375 | | | 23.79 | 27.57 | 0.863 | 15.87 | 778 | 920 |
| | 0.425 | | | 29.86 | 34.46 | 0.866 | 15.41 | 977 | 1150 |
| | 0.490 | | | 37.53 | 43.42 | 0.865 | 15.67 | 1228 | 1449 |
| 7 | 0.375 | 0.3 | 61.8 | 10.32 | 12.04 | 0.857 | 16.70 | 773 | 920 |
| | | | 42.6 | 14.96 | 17.47 | 0.856 | 16.79 | 772 | 920 |
| | | | 35.4 | 18.24 | 21.02 | 0.868 | 15.25 | 782 | 920 |
| | | | 29.4 | 22.82 | 25.32 | 0.902 | 10.92 | 813 | 920 |
| | | | 25.2 | 32.39 | 29.53 | 1.097 | 8.80 | 989 | 920 |
| 8 | 0.490 | 0.3 | 61.8 | 16.01 | 18.97 | 0.844 | 18.48 | 1199 | 1449 |
| | | | 42.6 | 23.47 | 27.52 | 0.853 | 17.24 | 1211 | 1449 |
| | | | 35.4 | 28.46 | 33.11 | 0.859 | 16.37 | 1220 | 1449 |
| | | | 29.4 | 34.80 | 39.87 | 0.873 | 14.57 | 1239 | 1449 |
| | | | 25.2 | 46.87 | 46.52 | 1.008 | 0.75 | 1431 | 1449 |
| | | | | | Average | 0.912 | | | |

### The effects of salt content

The increase in salt content from 0.20 to 0.70% w/w generally showed a decrease in ΔT (Fig. 3c). At a flow rate of 12 L/h, the slope of the curve between the salt content data points is approximately linear ($r^2 > 0.9$) with a slope of -15°C/ %w/w. This is contrary to the popular notion that an increase in salt content will increase the dielectric properties and, therefore, the dielectric heating (Li and Barringer 1997). One explanation for

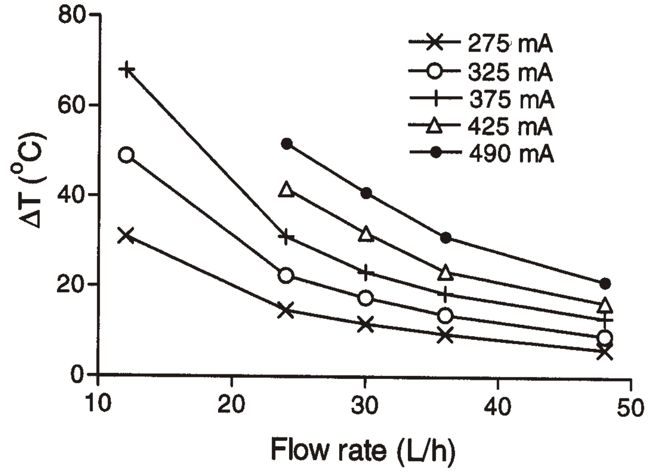


**Fig. 3a. Effect of flow rate on temperature increase (ΔT) during continuous heating of 0.27% guar solution (0.7% salt content) at different active currents.**

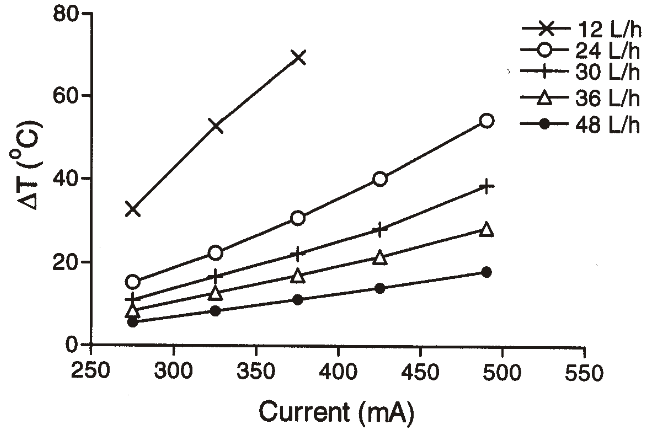


**Fig. 3b. Effect of active current on temperature increase (ΔT) during continuous heating of 0.27% guar solution (0.45% salt content) at different flow rates.**

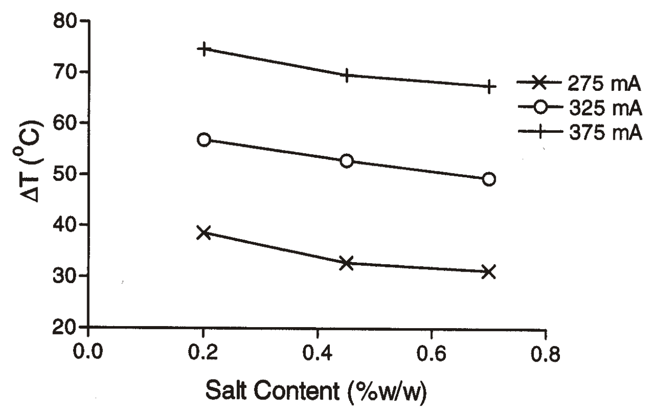


**Fig. 3c. Effect of salt content on temperature increase (ΔT) during continuous heating of 0.27% guar solution at different active currents (flow rate = 12 L/h).**

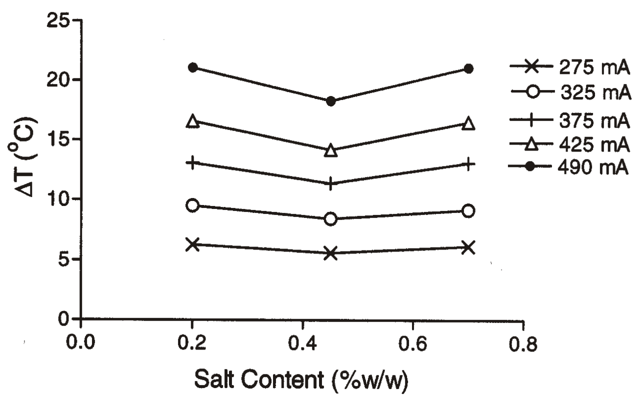


**Fig. 3d. Effect of salt content on temperature increase (ΔT) during continuous heating of 0.27% guar solution at different active currents (flow rate = 48 L/h).**

this phenomenon was proposed by Hasted et al. (1948). They suggested that the dielectric constant of a product could be lowered by a concentrated salt solution as a result of the saturation of the dielectric in the neighbourhood of an ion.

However, as seen at 48 L/hr (Fig. 3d) where $r^2<0.093$, the linear relationship disappears as the flow rate increases. The effect of salt content is less significant and ΔT is more constant. This could be due to the higher temperatures reached at low flow rates which may break down the guar molecule. It is possible that the ions only link to the broken down molecules due to higher temperatures and therefore can proportionally affect the heating only at slower flow rates.

The variability in the ΔTs at high flow rates might be due to the formation of layers according to the "theory of two hydration stages." This theory was developed by Padua (1993), who observed that sucrose-filled agar behaved differently according to the concentration of sucrose. Solutions containing between 0-0.6 g/g of sucrose consisted of units of sugar molecules with attached eight pairs of water molecules rotating freely in the continuous water medium. The increase in dielectric loss factor for sucrose indicated that sucrose molecules stabilized the hydrogen bonded structure of water and dissipated electromagnetic energy more effectively. Solutions containing 0.6-1.2 g sucrose/g water consisted of sucrose which associated through water bridges and formed loosely held clusters. The decrease in the loss factor suggested that as sucrose increased, the water molecules participated in more than one hydrogen bond and hindered their rotational movement. A study on the physical chemistry and dielectric properties of guar is required to confirm either of the above theories. However, this is beyond the scope of the study.

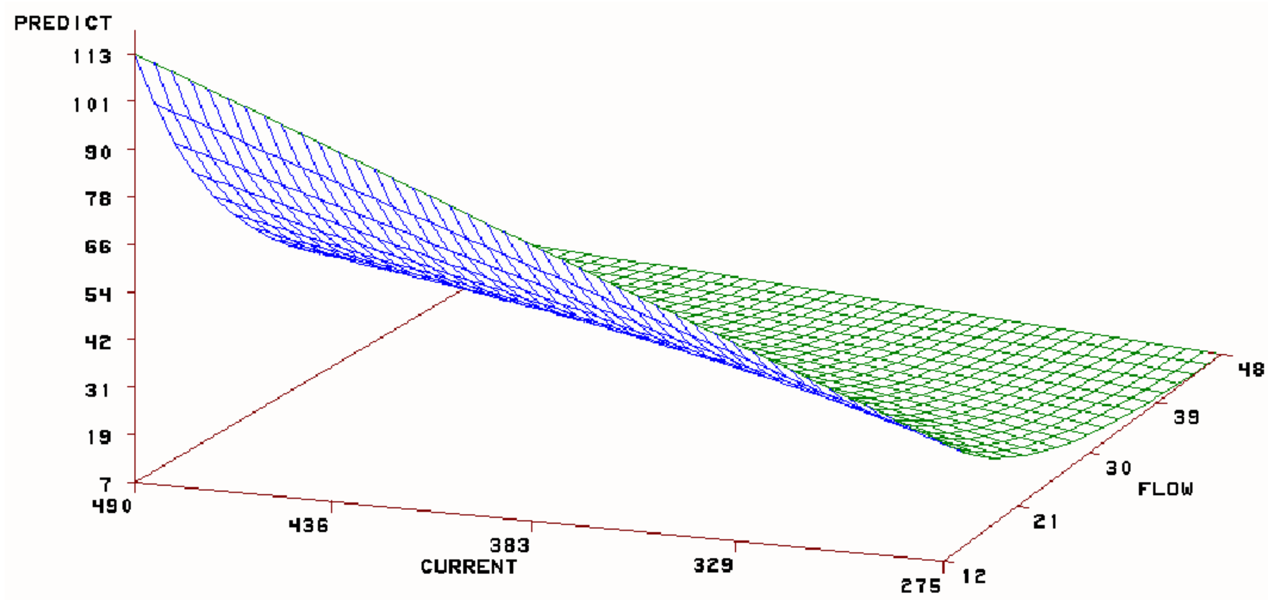


**Fig. 4. Fitted response surface for temperature increase (ΔT) during continuous heating of 0.27% guar solution with 0.2% salt.**

### Mathematical modelling

A unique empirical nonlinear multiple regression model was fitted for temperature increases as a function of salt content, flow rate, and active current:

$$\Delta T = c_0 + a \times salt + \frac{b}{flow^{1/2}} + c\exp\left(\frac{d}{flow^{1/2}}\right) \times current \quad (14)$$

where:

$c_0$ = 42.83,
a = -3.92,
b = -366.49,
c = 1.99, and
d = -0.49.

The regression coefficient ($r^2$) of the fit is 0.997. Number of data points used for the regression analysis was 207. As explained earlier, the effect of salt content is not significant, however there is a general trend that the ΔT decreases as the salt content increases. The fitted response surface for 0.2% salt content is given in Fig. 4. This model could be used to calculate the flow rate to obtain required ΔT at given active current.

### Temperature rise and power generation

Experimental ΔT and calculated ΔT (Eq. 8) along with correction factors (Eq. 10 ) and percent of errors (Eq. 11) for each test combination are given in Table 1. Estimated (Eq. 6) and experimental (Eq. 7) values of power generated are also given in Table 1. The estimated input power calculated from Eq. 6 and the power absorbed by the product calculated using Eq. 7 were very close. The value of the correction factor (Eq. 10) remained around 0.921 and the percent error for tests was below 20%, which was the loss anticipated for this equipment by the manufacturer (Strayfield 1993).

For a temperature rise (ΔT) of 86.57°C at the tested minimum flow rate (12 L/h) and maximum AcC (490 mA), for 0.27 % guar solution, ($\rho$ = 976 kg/m$^3$ and $C_p$ = 4450 J kg$^{-1}$ °C$^{-1}$, 0.2% salt), experimental $P_w$ was 1258.44 W (Table 1). Therefore, $P_{efficiency}$ (Eq. 9) was 39.33 %. This value is higher than the value (25-30%) reported by Houbon et al. (1991) for their RF unit. During continuous pasteurization using a heat regeneration system, a part of the heat could be recovered and used to heat the incoming cold liquid. Assuming 85% heat recovery in a plate heat exchanger during regeneration, the efficiency would be increased to 72.75%. Thus, only a small percentage of the energy input will be from RF heating**.** The results obtained from this and the previous studies (Awuah et al. 2002) will be used for further development of RF heating of liquid foods.

## CONCLUSIONS

Radio-frequency heating is affected by the flow rate with ΔT being inversely proportional to the flow rate. A linear relationship was found between the active current and ΔT. The results for the effects of salt content were inconclusive but did not seem to be significant within the range tested. The mathematical model developed to predict ΔT can be applied to the solutions studied under the specified operational conditions. Judging by the results, radio-frequency heating can provide enough heat to pasteurize viscous products and it is possible to obtain a maximum ΔT of 86°C in this RF unit under the tested conditions. The flow in the holding tube was laminar under the test conditions for 0.27% guar solution. The maximum power efficiency obtained was 39%.

## ACKNOWLEDGEMENT

The authors thank Dr. X. Lu for assistance in data analyses, M. Lefebvre for assistance in electrical and electronic modification, A. Saumure for assistance in machine work, and C. Defelice for rheological analysis. The authors also thank Drs. D.G. Mercer and H.S. Ramaswamy for reviewing the manuscript and providing constructive criticisms.

## REFERENCES

Anonymous. 1993. Radio frequency ovens increase productivity and energy efficiency. *Prepared Foods,* September: 125.

Awuah, G.B., H.S. Ramaswamy and P. Piyasena . 2002 Radio frequency (RF) heating of starch solutions under continuous flow conditions: Effect of system, and product parameters on temperature change across the applicator tube. *Journal of Food Process Engineering* 25(3): 201-223.

Bircan, C. and S.A. Barringer. 1997. Effect of viscosity on the dielectric properties. *IFT Annual Meeting Book of Abstracts* 75-10:219

Brown, G.H., C.N. Hoyler and R.A. Bierwirth. 1947. Theory and application of radio-frequency heating. New York, NY: D. Van Nostrand Inc.

Demeczky, M. 1974. Continuous pasteurization of bottled fruit juices by high frequency energy. *Proceedings of IV International Congress on Food Science and Technology.* IV: 11-20.

Geveke, D.J., M. Kozempel, O.J. Scullen and C. Brunkhorst. 2002. Radio frequency energy effects on microorganisms in foods. *Innovative Food Science & Emerging Technologies* 3: 133-138.

Hasted, J.B., D.M. Ritson and C.H. Collie. 1948. Dielectric properties of aqueous ionic solutions. Parts 1 and 2. *Journal of Chemical Physics* 16(1):1-21.

Houben, J., L. Schoenmakers, E. van Putten, P. van Roon and B. Krol. 1991. Radio-frequency pasteurization of sausage emulsions as a continuous process. *Journal of Microwave Power and Electromagnetic Energy* 26(4):202-205.

Koral, A.L. 1996. Proctor - Strayfield Magnatube Radio frequency Tube Heating System. Reading, UK: Strayfield.

Li, A. and S.A. Barringer. 1997. The effect of salt on the dielectric properties of ham at sterilization temperatures. *IFT Annual Meeting Book of Abstracts* 55-5:155.

Laycock, L., P. Piyasena and G.S. Mittal.2003.Radio frequency cooking of ground, comminuted and muscle meat products. *Meat Science* 65: 959-965.

McCormick, R. 1988. Dielectric heat seeks low moisture applications. *Prepared Foods* (9):139-140.

Orfeuil, M. 1987. *Electric Process Heating: Technologies/ Equipment/Applications*. Columbus, OH: Battelle Press.

Padua, G.W. 1993. Proton NMR and dielectric measurements on sucrose filled agar gels and starch pastes. *Journal of Food Sci*ence 58(3):603-604, 626.

Palmer, J.A. and Jones, V.A. 1976. Prediction of holding tube times for continuous thermal processing of power-law fluids. *Journal of Food Sci*ence 41: 1233-1234.

Piyasana, P. and R.C. McKellar. 1999a. Influence of guar on the thermal stability of *Listeria innocua, Literia monocytogenes*, and gamma-glutamyl transpeptidase during high-temperature short-time pasteurization. *Journal of Food Protection* 62 (8): 861-866.

Piyasena, P., and R. C. McKellar. 1999b. Selected physical properties of liquid egg products at pasteurization temperatures. *Journal of Food Processing and Preservation* 23: 153-168.

Rao, M.A. and R.C. Anantheswaran. 1982. Rheology of fluids in food processing. *Food Technology* 2:116-126.

Ryynänen, S. 1995. The electromagnetic properties of food materials: A review of the basic principles. *Journal of Food Engineering* 26: 409-429.

Sakiadis, B.C. 1984. Fluid and particle mechanics. In *Perrys' Chemical Engineers Hand Book,* eds. H. Perry and D. Green, 5:1-68. New York, NY: McGraw-Hill.

Strayfield. 1993. User Manual: 1.5 kW radio frequency tube heater. Reading, UK: Strayfield.

## NOMENCLATURE

| | |
|---|---|
| A | Cross sectional area of holding tube ($m^2$) |
| AcC | Active current applied across the electrodes (A) |
| $C_p$ | Specific heat of material to be heated (J $kg^{-1}$ $°C^{-1}$) |
| D | Diameter of the holding tube (m) |
| HTST | High-temperature short-time pasteurization |
| L | Length of the holding tube (m) |
| m | Consistency coefficient (Pa $s^n$) |
| n | Flow behaviour index |
| $N_{GRe}$ | Generalized Reynolds number |
| $P_{efficiency}$ | Power efficiency (%) |
| $P_s$ | Power supplied to the generator from the main (W) |
| $P_w$ | Power generated/absorbed during RF heating (W) |
| Q | Volumetric flow rate ($m^3$/s) |
| $RT_{min}$ | Minimum residence time in the holding tube (s) |
| T | Temperature (°C) |
| t | Temperature rise time (s) |
| V | Voltage applied across the electrodes (V) |
| $v_{av}$ | Average velocity [$4Q/(\pi D^2)$] (m/s) |
| $v_{max}$ | Maximum velocity (m/s) |
| $\Delta T$ | Temperature increase (°C) |
| $\rho$ | Density of the material to be heated (kg/$m^3$) |
| $\gamma$ | Shear rate ($s^{-1}$) |
| $\sigma$ | Shear stress (Pa) |